Numerical modeling and parametric sensitivity analysis of heat transfer and two-phase oil and water flow characteristics in horizontal and inclined flowlines using OpenFOAM

Nsidibe Sunday, Abdelhakim Settar, Khaled Chetehouna, Nicolas Gascoin

▶ **To cite this version:**

Nsidibe Sunday, Abdelhakim Settar, Khaled Chetehouna, Nicolas Gascoin. Numerical modeling and parametric sensitivity analysis of heat transfer and two-phase oil and water flow characteristics in horizontal and inclined flowlines using OpenFOAM. Petroleum Science, 2022, 10.1016/j.petsci.2022.10.008 . hal-03856796

HAL Id: hal-03856796
https://hal.science/hal-03856796

Submitted on 16 Nov 2022

HAL is a multi-disciplinary open access archive for the deposit and dissemination of scientific research documents, whether they are published or not. The documents may come from teaching and research institutions in France or abroad, or from public or private research centers.

L'archive ouverte pluridisciplinaire **HAL**, est destinée au dépôt et à la diffusion de documents scientifiques de niveau recherche, publiés ou non, émanant des établissements d'enseignement et de recherche français ou étrangers, des laboratoires publics ou privés.

Petroleum Science xxx (xxxx) xxx

Contents lists available at ScienceDirect

Petroleum Science

journal homepage: www.keaipublishing.com/en/journals/petroleum-science

Original Paper

Numerical modeling and parametric sensitivity analysis of heat transfer and two-phase oil and water flow characteristics in horizontal and inclined flowlines using OpenFOAM

Nsidibe Sunday*, Abdelhakim Settar, Khaled Chetehouna, Nicolas Gascoin

INSA Centre Val de Loire, Université Orléans, PRISME EA 4229, F-18020, Bourges, France

ARTICLE INFO

Article history:
Received 21 June 2022
Received in revised form
13 October 2022
Accepted 14 October 2022
Available online xxx

Edited by Xiu-Qiu Peng

Keywords:
Flow assurance
Flow pattern
Heat transfer
Flowlines
Two-phase flow
Global sensitivity analysis

ABSTRACT

Estimating the oil-water temperatures in flowlines is challenging especially in deepwater and ultra-deepwater offshore applications where issues of flow assurance and dramatic heat transfer are likely to occur due to the temperature difference between the fluids and the surroundings. Heat transfer analysis is very important for the prediction and prevention of deposits in oil and water flowlines, which could impede the flow and give rise to huge financial losses. Therefore, a 3D mathematical model of oil-water Newtonian flow under non-isothermal conditions is established to explore the complex mechanisms of the two-phase oil-water transportation and heat transfer in different flowline inclinations. In this work, a non-isothermal two-phase flow model is first modified and then implemented in the InterFoam solver by introducing the energy equation using OpenFOAM® code. The Low Reynolds Number (LRN) k-ε turbulence model is utilized to resolve the turbulence phenomena within the oil and water mixtures. The flow patterns and the local heat transfer coefficients (HTC) for two-phase oil-water flow at different flowlines inclinations (0°, +4°, +7°) are validated by the experimental literature results and the relative errors are also compared. Global sensitivity analysis is then conducted to determine the effect of the different parameters on the performance of the produced two-phase hydrocarbon systems for effective subsea fluid transportation. Thereafter, HTC and flow patterns for oil-water flows at downward inclinations of 4°, and 7° can be predicted by the models. The velocity distribution, pressure gradient, liquid holdup, and temperature variation at the flowline cross-sections are simulated and analyzed in detail. Consequently, the numerical model can be generally applied to compute the global properties of the fluid and other operating parameters that are beneficial in the management of two-phase oil-water transportation.

© 2022 The Authors. Publishing services by Elsevier B.V. on behalf of KeAi Communications Co. Ltd. This is an open access article under the CC BY-NC-ND license (http://creativecommons.org/licenses/by-nc-nd/4.0/).

1. Introduction

The exploitation of hydrocarbon resources in hostile and subsea deepwater surroundings has been driven by the continual increase in energy demand and depletion of already existing conventional oil-gas reserves (Oddie et al., 2003; Shahdi and Panacharoensawad, 2019; Sözbir, 2006). Two-phase flow in pipelines is usually experienced in the nuclear, chemical, and petroleum industries, mostly in the power generation, combustion systems, and crude oil transportation through inclined and horizontal pipelines (Bell et al., 2021; Jia et al., 2019). Transportation of this two-phase hydrocarbon through such environments (about 4–5 °C) which creates many flow assurance issues usually requires long flowlines (Guo et al., 2006; Shahdi and Panacharoensawad, 2019; Singh et al., 2017) as shown in Fig. 1. Flow assurance in the petroleum industry is one of the biggest problems bedeviling hydrocarbon production and this can cause serious challenges to subsea deepwater and ultra-deepwater field developments (Sunday et al., 2021; F. L. V. Vianna et al., 2009a). This type of surroundings is characterized by low seabed temperature and high hydrostatic pressures, which may affect the flow of the produced two-phase hydrocarbon fluids (oil, gas, and water) along the flowlines up to the processing facilities (Sunday et al., 2021; F. L. V. Vianna et al., 2009a). Also, the flowline has sections with different inclinations, usually

* Corresponding author.
E-mail address: nsidibe.sunday@insa-cvl.fr (N. Sunday).

https://doi.org/10.1016/j.petsci.2022.10.008
1995-8226/© 2022 The Authors. Publishing services by Elsevier B.V. on behalf of KeAi Communications Co. Ltd. This is an open access article under the CC BY-NC-ND license (http://creativecommons.org/licenses/by-nc-nd/4.0/).

Please cite this article as: N. Sunday, A. Settar, K. Chetehouna *et al.*, Numerical modeling and parametric sensitivity analysis of heat transfer and two-phase oil and water flow characteristics in horizontal and inclined flowlines using OpenFOAM, Petroleum Science, https://doi.org/10.1016/j.petsci.2022.10.008

Nomenclature

k	turbulence kinetic energy, m^2/s^2
Fs	body force in the axial direction, kg. m/s^2
g	gravity, m/s^2
p	pressure, kg/ms^2
U	velocity, m/s
T	temperature, K
c_p	specific heat capacity, J/(kg. K)
q''	heat flux, $w/(m^2. K)$
Pr	prandtl number, dimensionless
Re_{so}	superficial oil-phase Reynolds number
Re_{sw}	superficial water-phase Reynolds number
y^+	dimensionless distance to the pipe wall
G_k, G_b	productions of turbulent kinetic energy
Y_m	fluctuation dilation turbulence
S_k, S_ε	source terms
E, D	additional terms for dissipation stability
U_{so}, U_{sw}	superficial oil and water velocities, m/s

Greek letters

λ	thermal conductivity, w/(m. K)
ρ	density of the fluid, kg/m^3
α	volume fraction
μ	dynamic viscosity, m^2/s
μ_t	turbulence viscosity, m^2/s
θ	flowline inclination, deg
ε	turbulence dissipation rate, m^2/s^3
∇P	pressure gradient in streams direction, kg/m^2s^2 Γ_k effective diffusivity of k, m^2/s^2 Γ_ε effective diffusivity of ε, m^2/s^3 σ_k, σ_ε pressure gradient in streams direction, kg/m^2s^2 Γ_k effective diffusivity of k, m^2/s^2 Γ_ε effective diffusivity of ε, m^2/s^3 σ_k, σ_ε empirical turbulence model constant
Δ	altered range around the nominal value

Subscripts

o	oil-phase
w	water-phase
m	mean value
inlet	flowline inlet
outlet	flowline outlet
wall	flowline wall

Abbreviations

ANN	artificial neural network
HTC	heat transfer coefficient
LRN	low reynolds number

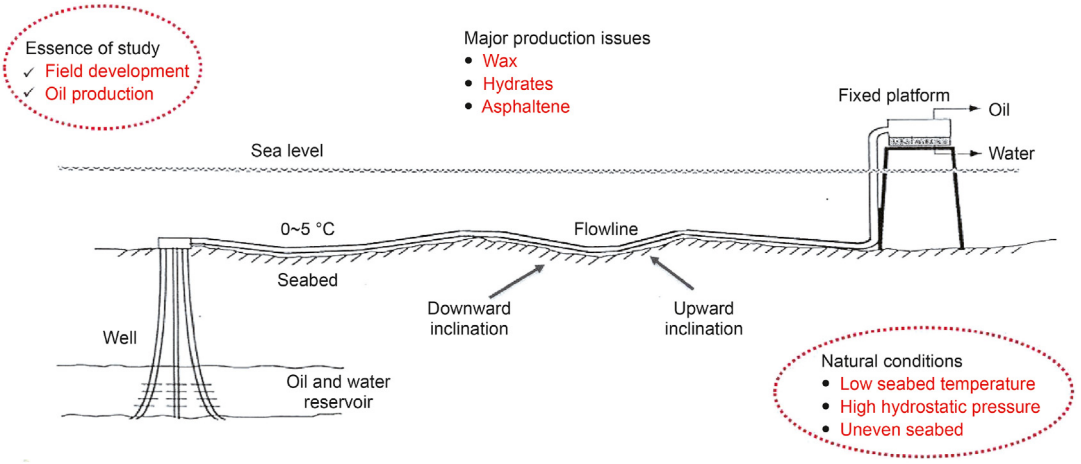

Fig. 1. Schematic representation of oil-water two-phase subsea production.

between −10° and +10° due to uneven seabed which affects the flow regimes (Amundsen, 2011) (Fig. 1). Therefore, a good grasp of the behavior of hydrocarbon fluids is important in oil production and field development.

The subsea heat management technique is a crucial ingredient to the successful operations of flow assurance in deepwater petroleum fields (Farshad et al., 2000; Sagar et al., 1991; Sunday et al., 2021; F. L. V. Vianna et al., 2009b). It is required during design to maintain the temperature of the fluid inside the flowlines well above the surrounding temperature. The accurate prediction of temperature and pressure is all-important for the prevention and remediation of flow assurance issues (Charles and Igbokoyi, 2012; Ji and Homan, 2007; Shang and Sarica, 2013; Sunday et al., 2021). One of the most significant measures in the design of subsea facility layout is the heat analysis of a subsea production system, which predicts the flowlines' temperature profile (Sunday et al., 2021; Toma et al., 2006; F. L. V. Vianna et al., 2009b). Heat analysis encompasses both steady-state and transient studies during different stages of the field's life and must serve as a standard design tool for heating systems or thermal insulation selection to avoid the formation of hydrate and wax (Ekweribe and Civan, 2011; Sözbir, 2006; Sunday et al., 2021; F. L. V. Vianna et al., 2009b).

The two-phase heat transfer process which changes with flow patterns, pressure drops, pipe orientations, and flow rates has long been of engineering interest (Adesina et al., 2011; Ekweribe and Civan, 2011; Sunday et al., 2022a). The oil-water flow structure is completely distinct from that of gas-oil flow and this distinction is ascribed to the small buoyancy effect and large momentum transfer capacity in the oil-water flows (Mehrotra et al., 2020; Trallero, 1995). Therefore, it is very important to develop new models for

the correct prediction of heat transfer and the different factors affecting oil-water two-phase flow phenomena during flowlines design, safety, and optimized operations.

Several technical and scientific research efforts have been established in the studies of heat transfer in pipelines. In the last five decades, most of the published two-phase heat transfer studies focused on gas-liquid in horizontal and vertical pipes (Amundsen, 2011; Moran et al., 2021; Shang and Sarica, 2013). Some were numerical investigations (Choi et al., 2013; Duan et al., 2013, 2015, 2014; Hetsroni et al., 1998; Kim and Ghajar, 2006) while many others carried out experimental studies on the effect of flow rates, flow patterns, and pipe orientations on the gas-liquid heat transfer process (Ghajar and Tang, 2010, 2007; Hetsroni et al., 2003; Kim and Ghajar, 2006; Trimble et al., 2002). The two-phase gas-oil flow structure is completely distinct from that of oil-water flow and this distinction is ascribed to the small buoyancy effect and large momentum transfer capacity in the oil-water flows (Adesina et al., 2011; Ekweribe and Civan, 2011; Mehrotra et al., 2020; Trallero, 1995). Therefore, it is very important to develop new models that correctly predict heat transfer and the different factors affecting oil-water two-phase flow phenomena during flowlines design, safety, and optimized operations.

Some theoretical models, empirical correlations, and experimental studies are reported for estimating the heat transfer of two-phase oil-water flow in pipelines (Legan and Knudsen, 1966; Leib et al., 1977; Shang and Sarica, 2013; Somer et al., 1973; Stockman and Epstein, 2001) which is limited when compared to gas-liquid heat transfer. Legan and Knudsen (1966) studied the turbulent heat and momentum transfer characteristics of unstable dispersion of oil droplets in water. But the authors' results were considered only applicable to water-oil dispersions within specified drop sizes, concentrations, and temperature ranges. Also, Legan and Knudsen were only able to predict the heat transfer coefficients and viscosity of a well-mixed oil in water dispersion by equation. The authors couldn't explain why the relative fluidity of both light oil and heavy dispersions decreases with temperature. Shang and Sarica (2013) developed a mathematical model that predicts the temperature profiles for two-phase oil-water stratified flows. The analytical model was verified by a single-phase heat transfer model and validated against experimental data. The authors reported that the simulated result from the analytical model was only validated for the water cut of 50% and verified for the water cuts of 0 and 100%. Generally, authors concluded the difficulty in predicting the heat transfer rate to the complexity of two-phase oil-water flow (Boostani et al., 2017; Li et al., 2018).

Flowline inclinations have become an area of concern during the development of fields and oil production due to the topography of the subsea seabed and this has prompted several researchers to investigate the relevance of pipeline inclinations on the hydrodynamic and thermal flow behavior. several authors have reported the effect of pipe inclination angles on flow patterns (Abduvayt et al., 2004; Lum et al., 2006; Oddie et al., 2003; Rodriguez and Oliemans, 2006), pressure drop (Kumara et al., 2010; Mukherjee et al., 1981; Rodriguez and Oliemans, 2006), liquid holdup (Abduvayt et al., 2004; Hamad et al., 2014; Kumara et al., 2010; Mukherjee et al., 1981; Rodriguez and Baldani, 2012; Rodriguez and Oliemans, 2006), drop velocity (Hamad et al., 2014), drag-reducing polymers (Abubakar et al., 2015), and HTCs (Boostani et al., 2017; Sunday et al., 2022b) in two-phase oil-water flows. Boostani et al. (2017) carried out an experimental investigation and artificial neural network (ANN) model to resolve the HTC, and flow pattern for oil-water flows in inclined and horizontal pipes. Due to the intrinsic complexity of multiphase flows, it has become arduous to develop a model that can accurately predict the HTC in oil-water flows (Boostani et al., 2017). To this end, no reported numerical model yet in the open literature has been employed to compute numerically the effect of different flowline inclinations and flow patterns on HTC for two-phase oil-water flow.

With the preceding review, the foremost contributions of our model relative to literature works are: (i) Providing detailed information about the complex two-phase oil-water flow field using an established non-isothermal mathematical model of oil-water flow. The model is capable of calculating velocity distribution, pressure gradient, liquid holdup, and temperature variation at the flowline cross-sections (ii) Evaluate the heat transfer coefficient and flow patterns for oil-water flows at downward inclinations of 4°, and 7° due to limited works focusing on downward flowline inclinations. (iii) Conduct a global sensitivity analysis to ascertain the impact of the different parameters on the performance of the produced two-phase hydrocarbon systems.

The overall objective of this paper is to study the intricate mechanisms of the two-phase oil-water transportation and heat transfer in the horizontal and inclined flowlines. Therefore, a non-isothermal two-phase heat transfer flow model that is vigorous enough to span the fluid combinations, flow patterns, flowline orientations, and flow rates is established to explore the effect of these issues. The LRN k-ε model is utilized to simulate the turbulence flow and to account for the near-wall treatment. This model takes into consideration the energy and LRN k-ε turbulence equations which are regarded as a more appropriate approach to the heat transfer phenomena and the Low Reynolds input. The model is validated by the experimental data found in the literature (Boostani et al., 2017). Subsequently, a global sensitivity analysis is conducted to determine the effect of the different parameters on the performance of the produced two-phase hydrocarbon systems for efficient fluid transportation. HTC and flow patterns for oil-water flows at different inclinations, velocity distribution, pressure gradient, liquid holdup, and temperature variation at the flowline cross-sections are simulated and analyzed in detail. This numerical model can become a reference for flow assurance in subsea deepwater and ultra-deepwater two-phase oil-water transportation, corrosion assessment, wax deposition, and pipeline optimization.

2. Mathematical model

Several studies on the hydrodynamics and thermal modeling of different flow behavior and flowline inclinations are performed, centering on computing the HTC, velocity and temperature distribution, pressure drop, liquid holdup, and flow patterns.

2.1. Governing equations

A supposedly non-isothermal two-phase Newtonian flow model has been established in this section. The governing equations comprise mass conservation, momentum conservation, and energy conservation equation.

From the preceding analysis, the mathematical models of non-isothermal two-phase Newtonian flow are detailed below:

2.1.1. Mass conservation equation

At the flowline cross-section in the axial direction, the total mass of the oil-water/gas-oil phases is constant. The conservation equation is shown as follows:

$$\frac{\partial \rho}{\partial t} + \nabla.(\rho U) = 0 \tag{1}$$

where ρ and U are the density of the velocity of the two-phase fluid.

2.1.2. Momentum conservation equation

Assuming an incompressible two-phase fluid flow, the Navier-Stokes equation in the axial direction of a fully developed flow is expressed as

$$\frac{\partial \rho U}{\partial t} + \nabla .\ (\rho UU) = \nabla P + \nabla .\ \left[\mu_{eff}\left(\nabla U + \nabla U^{T}\right)\right] + (\rho g sin\theta) + F_s \tag{2}$$

$$\frac{\partial \alpha}{\partial t} + \nabla .\ (\alpha U) + \nabla .(1-\alpha)\alpha U_r \Big) = 0 \tag{3}$$

where U is the velocity in the axial direction, ∇P is the pressure gradients in the stream's direction, g is the acceleration due to gravity, θ is the inclination angle, μ_{eff} is the effective dynamic viscosity which is the summation of the molecular and turbulent viscosity ($\mu + \mu_t$), U_r is the relative velocity between phases, α is the fluid volume fraction, and F_s is the body force in the axial direction.

The density and viscosity for two-phase oil-water flow are described in each cell by the volume fraction of the oil phase (α) as follows:

$$\rho = \alpha_w \rho_w + (1-\alpha_w)\rho_o \tag{4}$$

$$\mu = \alpha_w \mu_w + (1-\alpha_w)\mu_o \tag{5}$$

where subscripts o and w represent the oil and water phases, ρ and μ are the density and dynamic viscosity. The indicator function α is represented as:

$$\alpha \begin{cases} 1 & water \\ 0 < \alpha < 1 & two-phase\ flow \\ 0 & oil \end{cases} \tag{6}$$

2.1.3. Turbulence model

Because of the characteristics of turbulence in two-phase fluid flow, the turbulent fluctuation imposes additional momentum and energy transfer. Therefore, turbulent models are deployed to simulate momentum and energy transfer phenomena. The widely used turbulence model is the standard k-ε model by Launder and Spalding (1972). However, the model does not give accurate results close to the pipe wall for the high-Re approach. Thus the LRN k-ε model, by Launder and Sharma (1974) is introduced to account for the near-wall treatment by the addition of damping functions into the turbulent viscosity. The turbulent kinetic energy and dissipation are defined by:

$$\frac{\partial(\rho k)}{\partial t} + \nabla .(\rho k U_i) = \frac{\partial}{\partial x_j}\left[\Gamma_k \left(\frac{\partial k}{\partial x}\right)\right] + G_k + G_b - \rho\varepsilon - Y_m + S_k \tag{7}$$

$$\frac{\partial(\rho \varepsilon)}{\partial t} + \nabla .(\rho \varepsilon U_i) = \frac{\partial}{\partial x_j}\left[\Gamma_\varepsilon \left(\frac{\partial \varepsilon}{\partial x_j}\right)\right] + C_1 f_1 \frac{\varepsilon}{k}(G_k + G_b) - C_2 f_2 \rho \frac{\varepsilon^2}{k} + E + D + S_\varepsilon \tag{8}$$

where k is the turbulent kinetic energy, ε is the turbulent dissipation rate, $C_1 = 1.92$, and $C_2 = 1.3$ are the model constants for the LRN k-ε model, f_1, and f_2 are the functions specially employed for the near-wall treatment, G_k and G_b are the productions of turbulent kinetic energy, and Y_m is the fluctuation dilation incompressible turbulence. μ_t is the turbulent viscosity, Γ_k and Γ_ε are effective diffusivities of k and ε. E and D are additional terms to further stabilize dissipation and diffusion in the area of the walls, S_k and S_ε are the source terms.

$$\Gamma_k = \left(\mu_m + \frac{\mu_t}{\sigma k}\right) \tag{9}$$

where Γ_k is the effective diffusivity of k, and σ_k is the empirical turbulence model constant. $\sigma_k = 1$ for the LRN $k \sim \varepsilon$ model and μ_t is the turbulent viscosity.

$$\Gamma_\varepsilon = \left(\mu_m + \frac{\mu_t}{\sigma \varepsilon}\right) \tag{10}$$

where Γ_ε is the effective diffusivity of ε, σ_ε is the empirical turbulence model constant. For the LRN $k \sim \varepsilon$ model $\sigma_\varepsilon = 1.3$.

$$\mu_t = \frac{f_\mu C_\mu\ \rho k^2}{\varepsilon} \tag{11}$$

where ρ is the density of the fluid, and $C_\mu = 0.09$ is the model constant. f_μ is the function utilized for the near-wall treatment.

2.1.4. Energy conservation equation

The heat-transfer process especially with the turbulent flow is valuable for both engineering and due to its occurrence in numerous industrial applications. Thus energy equation is added to the governing equations. Assuming a quasi-transient state in which axial heat conductive heat effect is neglected, no added source term in the energy equation. The energy equation is shown as:

$$\frac{\partial T}{\partial t} + \nabla_z .(\rho C_p U T) = \nabla_x .\left[\frac{\mu_a\ C_p}{Pr}(\nabla_x\ T)\right] + \nabla_y .\left[\frac{\mu_a\ C_p}{Pr}(\nabla_y T)\right] \tag{12}$$

where T is the temperature of the two-phase fluid, Cp is the specific heat capacity of the two-phase fluid, and Pr is the Prandtl number.

$$Pr = C_p \frac{\mu_a}{\lambda} \tag{13}$$

where Pr is the Prandtl number, λ and μ_a are the thermal conductivity and kinematic viscosity of the two-phase fluid respectively.

2.2. Boundary conditions

Fig. 2 describes the computational domain of the two-phase oil-water flow employed for the current study. The flowline is initially deemed to be filled with water. At the onset of the simulation (time = 0), an equal volume fraction of oil-water was infused at the inlet domain of the flowline with different superficial inlet velocities, the outlet permits the mixed flowing fluids to come out of the domain with a pressure of zero, the fluids at the wall was assumed

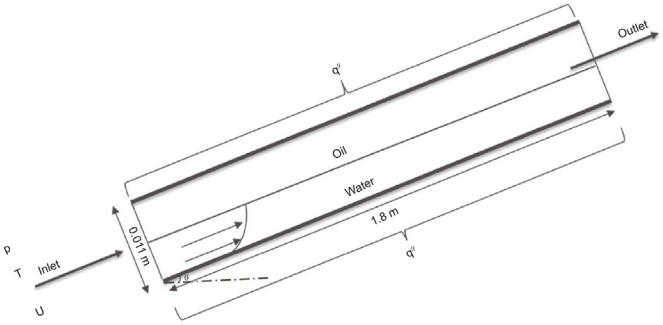

Fig. 2. A simplified domain of the two-phase oil-water flow.

as a no-slip condition with zero velocity, and the symmetry-plane boundary condition was used in the longitudinal pipe section (X-Z plane). A uniform wall heat flux value ranges from 15,100–24,800 W/m^2 and at atmospheric pressure (room temperature of about 25 °C). Table 1 gives the boundary conditions for all simulations.

3. Numerical method and parametric sensitivity analysis

OpenFOAM v.7 was used to simulate different two-phase flow cases. The two-phase flow is calculated by using the new solver based on the VOF approach (Hirt and Nichols, 1981). Turbulence effects and their influence on the flow were performed for all simulations using different RANS models. The LRN k-ε turbulence model supporting the low $y+$ approach was used for the grid-sensitive studies for accurate near-wall treatment with an automatic switch from a wall function to LRN formulation by grid spacing (Wilcox, 2006).

3.1. Model geometry and mesh

A 3D flowline was constructed with a diameter and length of 0.011m and 1.8 m respectively, symmetry boundary condition's domain was chosen aimed at reducing the computational cost. The mesh consisting of structured hexahedral cells is bounded by three types of boundary faces (inlet, outlet, and wall), as seen in Fig. 3. Both geometry and the structured mesh were created by the blockMesh utility in OpenFOAM.

3.2. Discretization methods

Discretization of the transport equation is executed using the Finite Volume Method. The Euler scheme is used for temporal and time discretization and spatial discretization is a standard second-order scheme. The convective term is discretized with a second-order upwind scheme. As for the diffusion term, a second-order corrected scheme is applied.

3.3. Solutions procedure

Two-phase fluid flow is a complex flow system with hydrodynamic and thermal coupling, where the numerical solution of governing equations is conducted individually for each phase. The velocity, temperature, viscosity, pressure gradient, and shear rate calculation of the fluid need to be iterated until all converges. A computer code is established for the computation of the governing equations and a flow chart algorithm is described in Fig. 4. The solution is explained in the following steps below:

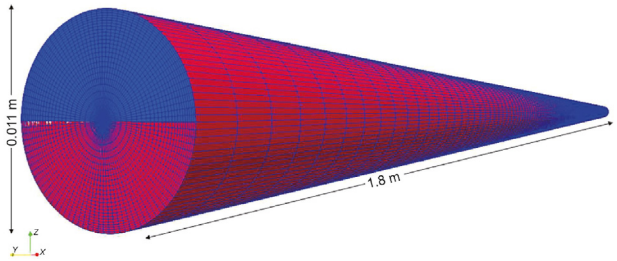

Fig. 3. A mesh inlet section for two-phase oil (blue) and water (red) flow.

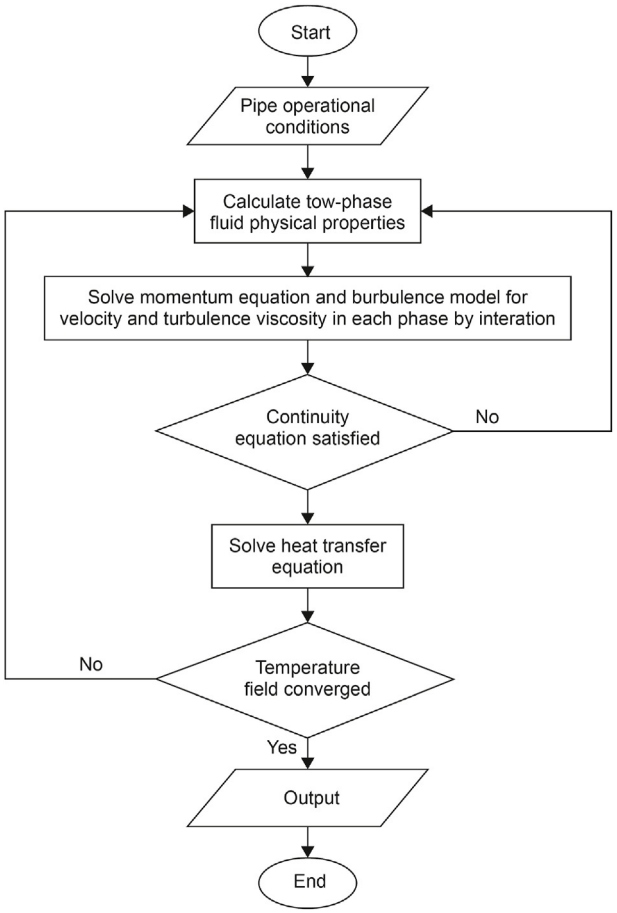

Fig. 4. The flow chart of the program.

Table 1
Boundary conditions.

Variables	Inlet	Outlet	Wall
U	$U_{w,o} = U_{w,\&o,inlet}$	$\frac{\partial U_{w,o}}{\partial x} = 0$	$U_{w,\&o,wall} = 0$
T	$T_w = T_o = T_{inlet}$	$\frac{\partial T}{\partial x} = 0$	$h = (T_{wall} - T_m) = \lambda \frac{\partial T}{\partial r}$
$p - \rho gh$	$\frac{\partial P}{\partial x} = 0$	$P_{w\&o,outlet} = 0$	$\frac{\partial P}{\partial z} = 0$
k	$k_{w,o} = k_{w,\&o,inlet}$	$\frac{\partial k_{w,o}}{\partial x} = 0$	$k_{w,o,g} = k_{wall}$
μ_t	$\mu_{t,cal} = 0$	$\mu_{t,cal} = 0$	$\mu_{t,kwallfunc} = \mu_{t,wall}$
ε	$\varepsilon_{w,o} = \varepsilon_{inlet}$	$\frac{\partial \varepsilon_{w,o}}{\partial x} = 0$	$\varepsilon_{wallfunc} = \varepsilon_{wall}$

(1) Flowline operations conditions are set such as flowlines length and diameter, inlet and surrounding temperature, heat flux, and two-phase fluid flow rates.
(2) Estimate the two-phase physical properties. The liquid physical properties are calculated.
(3) The velocity, kinetic energy, and dissipation rate are acquired from the momentum conservation equation and turbulence model resolved for each phase by iteration until the convergence criterion is achieved. If it is converged, then proceed to step (4); otherwise, go back to step (2).
(4) The temperature field is got from the heat-transfer equation, and updates from the physical properties. If it is converged, then proceed to output the result, the calculation terminates, otherwise, return to step (2).

3.4. Grid independence study

To assess mesh fineness on the solution to obtain minimum mesh density with good accuracy. Five meshes were created with the blockMesh tool for the mesh sensitivity analyses. The mesh data are summarized in Table 2, and the outcome of the comparisons of the HTCs values at different flow patterns between the experimental data and the different mesh sizes is shown in Fig. 5.

The relative error between the experimental and numerical HTCs decreases as the cell numbers increase both normal to the pipe wall and flow direction until obtained results give an acceptable margin. The relative error and calculation time range from 39.75% to 1.80% and 258 h−558 h for plugs of water in oil (Fig. 5a), 45.58.75%−1.76% with 205 h−425 h for stratified flow with a mixed interface (Fig. 5b), 50.29%−2.42% and 190 h−323 h for dispersion of water in oil & oil in water (Fig. 5c), and 48.13%−2.13% and 65 h−208 h for dispersion of oil in water (Fig. 5d). It is observed that there is no noticeable difference between mesh 4 and mesh 5 with regard to the relative error which yields satisfactory HTCs results but there is a substantial difference in computational time. The relative errors for meshes 4 and 5 are from 3.01% to 1.81% while the computational time is from 449 h to 558 h for plugs of water in oil, 2.72%−1.77% with a calculation time of 360 h−425 h for stratified flow with a mixed interface, 3.58%−2.42% and 252 h−323 h for dispersion of water in oil & oil in water, 2.67%−2.13% and 167 h−208 h for dispersion of oil in water. Therefore, Mesh 4 is chosen for further investigation as a compromise between computational cost and accuracy.

3.5. Models validation

The proposed model is validated by the experimental investigation of Boostani et al. (2017). In this work, the authors studied the heat transfer coefficient of oil-water flow in horizontal and inclined (+4°, +7°) pipes. The superficial Reynolds number of the water-phase, Re_{sw} was maintained at 6772, while the superficial Reynolds numbers of the oil-phase Re_{so} varied at intervals. To validate the studied results, the numerical results of flow patterns and HTCs for oil-water two-phase flow at different flowline inclinations are compared with experimental data. Therefore, the thermohydraulic calculations are both tested and established.

Fig. 6 gives the oil-water flow pattern maps for different flowline orientations (-7°, -4°, 0°, +4°, +7°), classified in line with the definitions of Boostani et al. (2017) and Oddie et al. (2003). The observed flow patterns are stratified flow (ST), stratified flow with a mixed interface (ST & MI), plugs of oil in water (Po/w), plugs of water in oil (Pw/o), dispersion of water in oil & oil in water (Dw/o & o/w), and dispersion of oil in water (Dw/o), annular (AN) flows. The oil-water physical properties are described in Table 3.

To verify the ability of the calculation code to reproduce the experimental measurements of Boostani et al. (2017), the highlighted cases (dashed lines) in Fig. 6 are simulated. Table 4 illustrates a results comparison between numerical and measured flow patterns visualized at different Re_{so} (≈450−3750) and Re_{sw} kept at 6772. The non-isothermal two-phase flow model predicted the observed flow patterns of oil-water flow very reliably. For instance, in horizontal flow, the performance of the model was remarkably good for all Po/w, ST & MI, Dw/o & o/w, and Dw/o are predicted correctly by the 3D model.

Fig. 7 describes the comparison between the numerical and measured HTC values under various Re_{so} of about 450−3750 when the Re_{sw} is 6772 at different flow inclinations (0°, +4°, +7°). The numerical HTC results are slightly different from the experimental values as the flow patterns changes from Po/w to Dw/o. The relative errors between the calculated HTC and experimental results at Re_{so} of approximately 450, where there is a decrease of HTC due to flow pattern change from Po/w to ST & MI is roughly 1% for the 3-D model. At a Re_{so} of around 1280, the relative error for the horizontal flow where the HTC value is higher than the inclined flow is ≈ 2% for the 3-D model. Also at a Re_{so} of around 3300, Dw/o is only observed within this region because of higher turbulence forces and the relative error is around 3%. In summary, the results of the relative errors obtained between Boostani's experimental data and the numerical model are within 3%, which demonstrates the model's accuracy as shown in Fig. 8.

3.6. Parametric sensitivity analysis technique

3.6.1. Sensitivity analysis theory

A good understanding of the behavior of two-phase hydrocarbon fluids is key during field development and production. Hence, the performance of the hydrocarbon transportation system through surroundings with low seabed temperature and high hydrostatic pressures depends on parameters such as (1) Flowline geometry-Inclination, diameter, roughness; (2) Hydrodynamic fluid behavior-velocity, slip ratio, pressures, flow pattern, holdup; (3) Thermophysical properties- Temperature, density, viscosity, specific heat capacities, thermal conductivities, heat flux, etc. It has become difficult to study these parameters knowing well that most of them can be arduous to accurately measure or predict. Consequently, sensitivity analysis is essential to determine beforehand the importance of the input parameters acting individually or in combination and must be factored in during field and laboratory studies.

Sensitivity analysis is widely embraced as a necessary aspect of good modeling practice, and amongst the reason for using sensitivity analysis are: to identify factors that are unimportant to model output and can be removed from further analysis; to identify the factors that have the most impact on model output; to determine if a model reproduces know effects upon the processes it is simulating; to identify factors that may require more research to enhance confidence in model output; to discover the optimal regions within the parameter space for use in calibration studies; to determine which, if any, factors or groups of factors interact with each other; to establish regions in the space of inputs where the variation in model output is maximum; finally to demonstrate if model predictions are robust to plausible variations in input factors.

Table 2
Mesh statistics for the grid independence study.

Geometry	Mesh configuration	Mesh1	Mesh2	Mesh3	Mesh4	Mesh5
3D case	Cells	90000	150000	250000	390000	570000

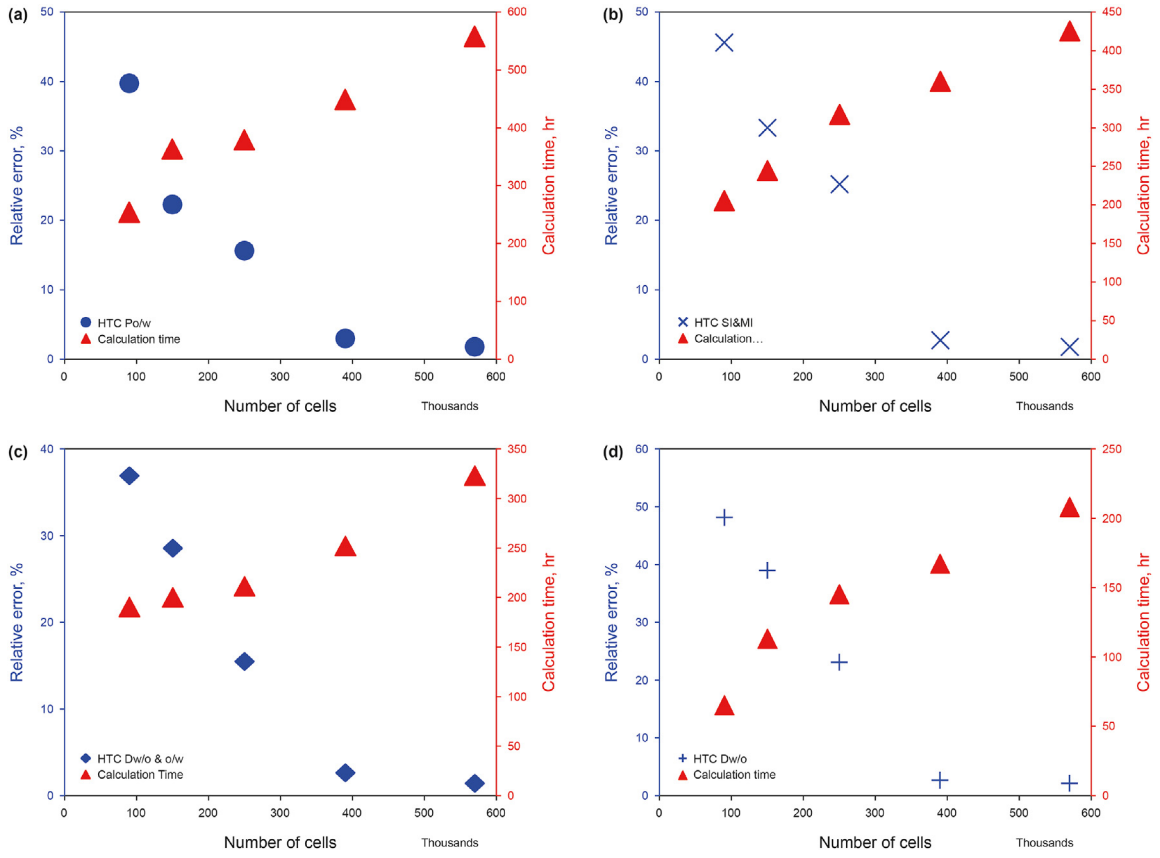

Fig. 5. Graphical description of the mesh sensitivity analysis for different flow patterns (**a**) Po/w, (**b**) SI & MI, (**c**) Dw/o & ow, and (**d**) Dw/o flows.

Table 3
Physical properties of oil and water.

Parameter	Value	Unit
Oil density	798	kg/m^3
Water density	1000	kg/m^3
Oil kinematic viscosity	3.1203×10^{-5}	m^2/s
Water kinematic viscosity	1×10^{-6}	m^2/s
Oil-specific heat	2050	m^2/s^2 K
Water-specific heat	4184	m^2/s^2 K
Oil Prandtl number	37.811	
Water Prandtl number	6.90	
Oil-water Interfacial tension	3.7×10^{-2}	N/m

Different sensitivity analysis techniques exist in a wider range of scientific investigations (Hall et al., 2009). Saltelli et al. (2004) reported three major groups:

- Screening: a qualitative sensitivity analysis method
- Global: quantitative analysis (variance-based) methods that vary all parameters examined in their variation ranges.
- Local: a quantitative analysis (factorial design) method varies parameters successively around nominal values.

For this study, the local sensitivity analysis is chosen as the most appropriate technique due to:

- The number of input parameters,
- The computational cost of running the model,
- The settling for the analysis, and
- Analysis time available for sensitivity analysis.

Local sensitivity analysis of the two-phase flow in the flowline using the thermohydraulic model is conducted using the factorial design method. The local sensitivity analysis involves the uniform distribution of input data by random sampling and it also allows for the interaction between two or more input parameters to be investigated. Decision makers who utilize thermohydraulic model results can justly request thorough analysis results to reasonable variations in the model inputs. This information can be employed to target data acquisition and engineering design decisions effectively by identifying key parameters that impose the greatest influence on system performance.

3.6.2. Factorial design

The factorial design method explores small changes around nominal value (s). The required total number of simulations is 2^n, where n is the number of input parameters, and each input parameter is altered in a range of 10% by $+\Delta$ and $-\Delta$ around the nominal value (s) (Akridiss Abed et al., 2020). The response of the system would depend on the results of the simulations. In our case, six input parameters have been selected for the sensitivity analysis. These parameters are flowline inclination (θ), the minimum and maximum superficial oil velocity (U_{so}), minimum and maximum superficial water velocity (U_{sw}), the thermal conductivity of oil (λo), the thermal conductivity of water (λw), and the wall heat flux ($q"$). The linear regression model using the factorial design method is expressed as:

$$y_{\dot{o}} = c_0 + \sum_{j=1}^{n} c_j x_j + \sum_{j=1}^{n} \sum_{k=j+1}^{n} c_{jk} x_j x_k + \cdots + c_{123 \to n} \prod_{j=1}^{n} x_j \qquad (14)$$

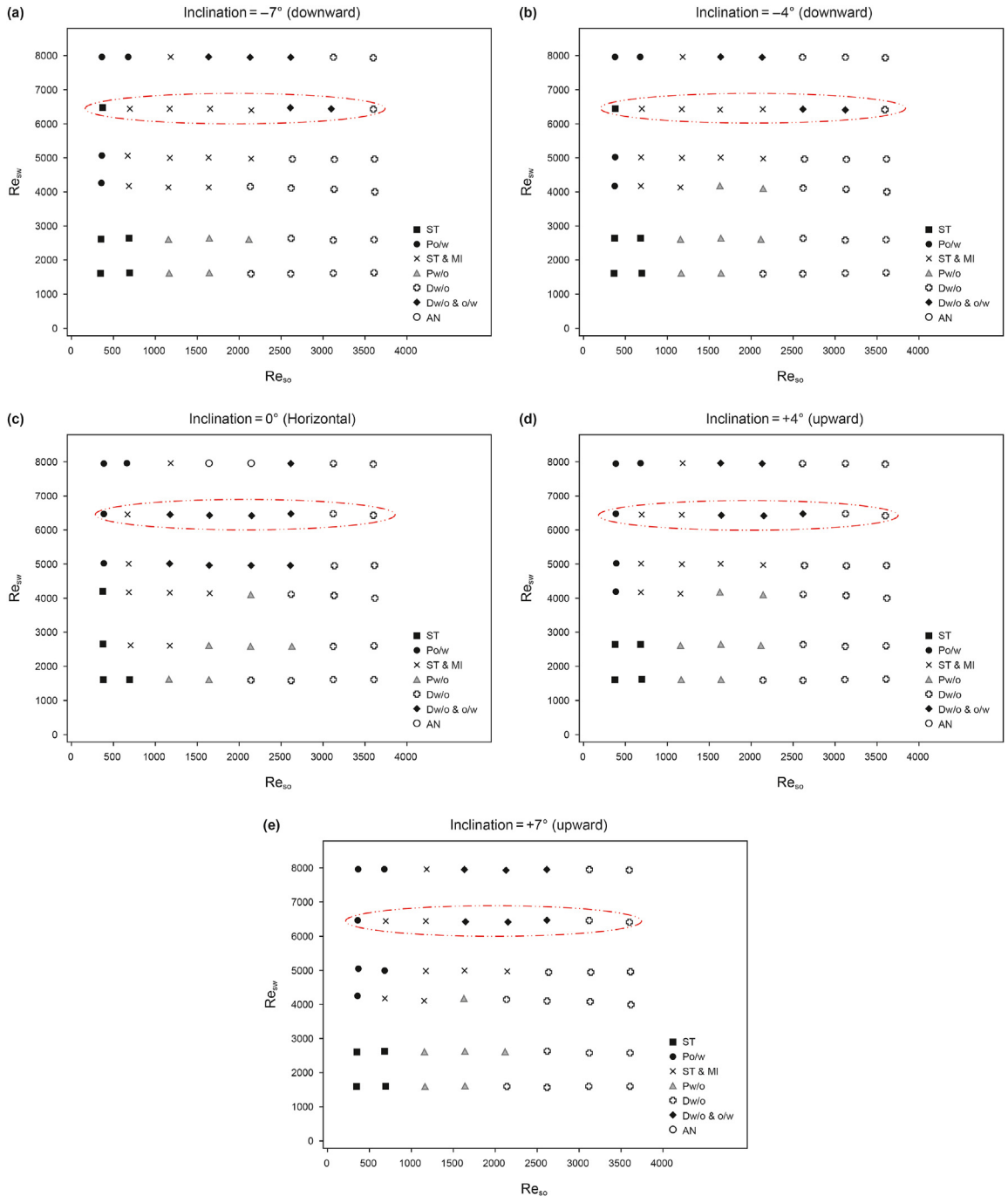

Fig. 6. Flow patterns map for oil-water two-phase flow inclinations system with highlighted simulation points.

where n is the number of input parameters, $y_{\dot{o}}$ is the estimated response by the model, C is the coefficient of the polynomial, and x_j is the j^{th} input parameter.

Therefore, with six input parameters, Eq. (14) becomes:

$$y_{\dot{o}} = c_0 + \sum_{j=1}^{6} c_j x_j + \sum_{j=1}^{6} \sum_{k=j+1}^{6} c_{jk} x_j x_k + \cdots + c_{123456} x_1 x_2 x_3 x_4 x_5 x_6 \tag{15}$$

Each of the six input parameters of the model reported above is estimated at 10% (+1) higher and 10% (−1) lower around each nominal value (s). As a result, 64 (2^6 factorial) simulations must be executed. $y_{\dot{o}}$ can be written into the matrix form from Eq. (15) as shown.

$$y_{\dot{o}} = cX \tag{16}$$

The coefficient of the matrix which determines the relevance of each input parameter becomes

$$c = X^{-1} y_{\dot{o}} \tag{17}$$

The established numerical model was utilized for the predictions by applying the sensitivity analysis technique.

Table 4
Comparison of present work and experimental oil-water flow patterns.

Flowline Inclinations					
0°		+4°		+7°	
Exp	3D Predict	Exp	3D Predict	Exp	3D Predict
Po/w	Po/w	Po/w	Po/w	Po/w	Po/w
ST & MI	ST & MI	ST & MI	ST & MI	ST & MI	ST & MI
Dw/o & o/w	Dw/o & o/w	ST & MI	ST & MI	ST & MI	ST & MI
Dw/o & o/w	Dw/o & o/w	Dw/o & o/w	Dw/o & o/w	Dw/o & o/w	Dw/o & o/w
Dw/o & o/w	Dw/o & o/w	Dw/o & o/w	Dw/o & o/w	Dw/o & o/w	Dw/o & o/w
Dw/o & o/w	Dw/o & o/w	Dw/o & o/w	Dw/o & o/w	Dw/o & o/w	Dw/o & o/w
Dw/o	Dw/o	Dw/o	Dw/o	Dw/o	Dw/o
Dw/o	Dw/o	Dw/o	Dw/o	Dw/o	Dw/o

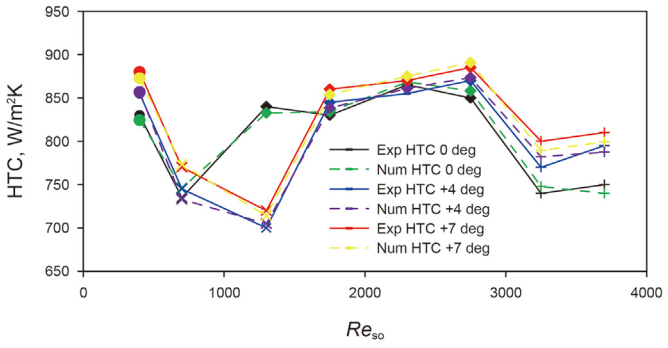

Fig. 7. The HTC variation at horizontal and inclined flowline as a function of Re_{so}.

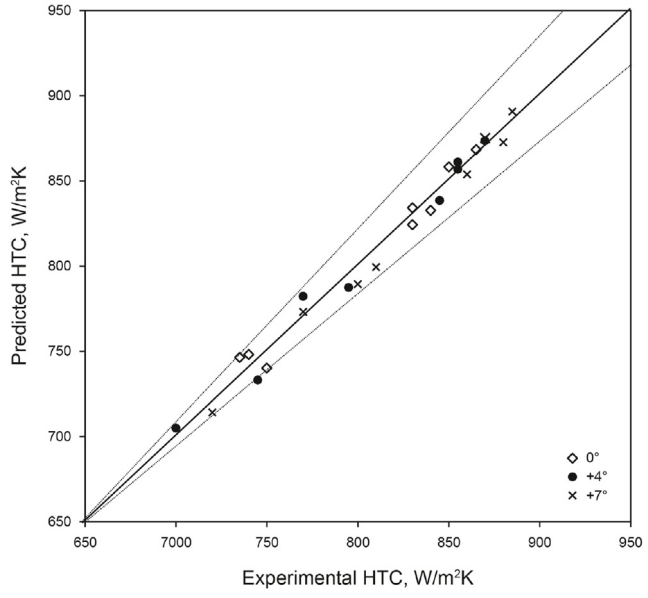

Fig. 8. The plot of the predicted values with a numerical model versus experimental values for all data and all studied inclined positions.

4. Results and discussion

4.1. Sensitivity analysis result

The global sensitivity analysis method discussed in the previous section is then applied to the validated numerical model. The minimum and maximum superficial liquid velocities were utilized to determine the flow pattern boundaries. ST flow pattern is selected for minimum U_{so} and minimum U_{sw}, and the Dw/o flow pattern is chosen for maximum U_{so} and maximum U_{sw}. The results are presented in decreasing order by using the Pareto chart to describe the importance of each parameter and their interactions. Table 5 shows the selected nominal values and their respective variations from the input parameters of Boostani's experimental work employed for the sensitivity analysis.

4.1.1. ST flow pattern

This flow pattern represents the region of the minimum possible values for both superficial oil and water velocities in horizontal flowlines as shown in Table 5. Fig. 9 describes the effect of each parameter and its interactions with the outlet temperature. It is observed that the outlet temperature (T_{outlet}) is mostly affected by the flowline inclination (θ), afterward the superficial oil and water velocities (U_{so} & U_{sw}), the thermal conductivity of oil (λ_o), and wall heat flux (q'') for an ST flow pattern system. The effect of the inclination angle, θ on the variation of temperature is entrenched because θ influences the flow regime and in turn determines the heat transfer. U_{so} and U_{sw} have a great influence on the fluid temperature positively since a slowly moving fluid retains heat. λ_o and the q'' are also positive on the outlet fluid temperature because they enhance the thermal behavior of the fluid. On the parameters' combination, θU_{sw} are the most influencing interactions on the fluid temperature. θU_{so} has the most inverse influence on the outlet fluid temperature.

4.1.2. Dw/o flow pattern

This region shows the maximum values feasible for both superficial oil and water velocities in the horizontal flowline as expressed in Table 5. The result of the effect of inputs parameters and their interaction on the outlet temperature is expressed in Fig. 10. It is noticed that the two-phase oil-water outlet temperature (T_{outlet}) is highly influenced by θ, then U_{sw}, λ_o, and q''. The effect of the inclination angle, θ on the outlet temperature of the fluid is established since θ affects the fluid flow regime which influences the heat transfer. U_{sw} has an inverse influence on the fluid temperature since dispersed water dissipates heat quickly as it flows. λ_o, and q'' are also positive on the fluid temperature for the reason that they enhance the thermal behavior of the fluid. For the parameters' combination, θU_{sw} and θU_{so} interactions have little influence on the fluid temperature.

As a result of this analysis, the most important parameters affecting the fluid temperature for the ST flow pattern are flowline inclination (θ), superficial oil and water velocities (U_{so} & U_{sw}), the thermal conductivity of oil (λ_o), and the wall heat flux (q''). For the Dw/o flow pattern, the parameters are the flowline inclinations, the thermal conductivity of oil (λ_o), wall heat flux (q''), and the superficial oil and water velocities U_{sw}. This reaffirms two-phase heat transfer as dependent on the flowline inclinations, hydrodynamic, and thermal behavior of the flow. As seen below, the model can

Table 5
Input parameters of ST and Dw/o flow patterns for the sensitivity analysis.

Input Parmeter	Flow Pattern	Minimum (10% below nominal)	Nominal value	Minimum (10% above nominal)	Unit
θ	ST, Dw/o	−10	0	+10	deg
Usw	ST, Dw/o	0.09, 0.90	0.1, 1	0.11, 1.10	m/s
Uso	ST, Dw/o	0.09, 0.90	0.1, 1	0.11, 1.10	m/s
λw	ST, Dw/o	0.538	0.598	0.658	w/(m. K)
λo	ST, Dw/o	0.149	0.135	0.149	w/(m.K)
q''	ST, Dw/o	165333.333	183703.704	202074.074	w/(m^2.K)

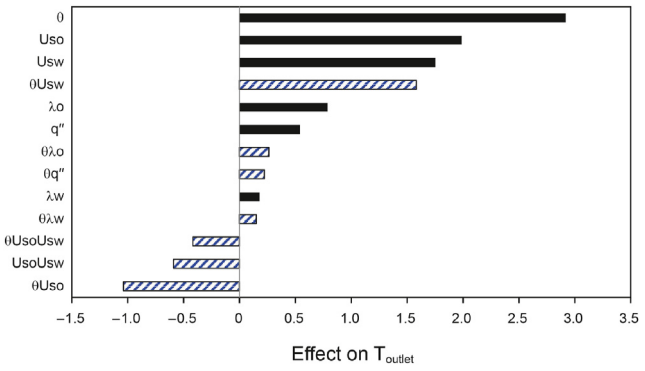

Fig. 9. Factor effect of the parameters affecting the fluid temperature for ST flow.

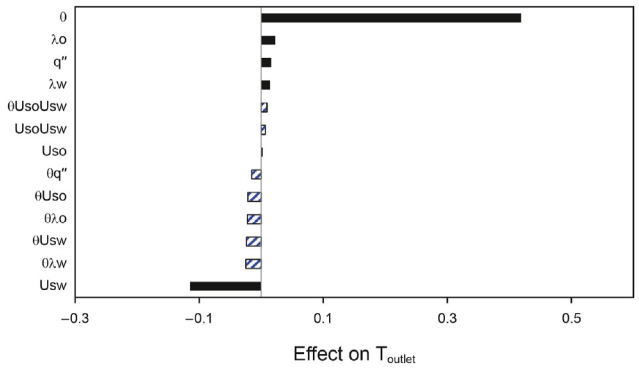

Fig. 10. Factor effect of the parameters affecting the fluid temperature for DW flow.

provide reasonable predictions of the hydrodynamic behavior of the oil-water flow, there is good accuracy for the prediction of flow pattern, pressure drop, liquid hold, and velocity distribution. In the following subsections, the effect of flowline inclinations on the hydrodynamic and thermal behaviors will be investigated deeply in order to determine the limitation range in terms of flowline inclinations to finally ensure efficient crude oil transportation.

4.2. Effect of flowline inclinations on the hydrodynamic behavior

4.2.1. Flow pattern and liquid fraction

4.2.1.1. Flow pattern. Table 6 recapitulates the obtained flow patterns for different flowline inclinations (-4°, -7°, 0°, +4°, +7°). For Re_{so} values of about 450−2750 and Re_{sw} maintained at 6772, it is observed that the change of flowline inclination angle leads to a change in the flow pattern transition boundaries from Po/w, ST & MI to Dw/o & o/w. Po/w is formed at low Re_{so} (≈450) and high Re_{sw} (6772) due to buoyant forces acting to settle the oil droplet, increasing the Re_{so} forms ST & MI with droplets at one or both sides of the interface observed, and a further increase in Re_{so} (≈2750) gives rise to Dw/o & o/w flow regime by the turbulent interfacial forces forcing droplets to spread all over the flowline. As seen in Table 6, for the horizontal situation the flow pattern of Dw/o & o/w was mostly noticed over a wider range of oil and water flow rates than for the downward and upward flowline inclinations. When the flowline was inclined from horizontal to upward inclinations of 4° and 7°, the observed flow pattern was similar to horizontal flow except at Re_{so} of around 1280 where the flow pattern is ST & MI. This is due to a reduction in turbulence forces in ST & MI created by the gravitational forces which hinder the denser water phase leading to a high liquid holdup. As the flowline was inclined from horizontal to downward inclined positions 4° and 7°, the flow pattern is observed to be mostly ST & MI with Po/w and Dw/o & o/w only observed respectively at low and high Re_{so}. Varying the inclination angle downward reduces liquid holdup and the gravitational forces, which are most pronounced at upward inclinations and tend to decelerate the denser water phase in the upward direction. Water is the fastest-moving phase during the downward flow and it reduces the holdup.

4.2.1.2. Liquid holdup. The Liquid Holdup (HL) is the in-situ volume fractions of the oil-water phases flowing in the flowline. The input volume fractions may be different from the in-situ volume fractions and this behavior describes holdup. HL is simply the fraction of a particular fluid present in the interval of a pipe, and its accurate determination is useful to calculate frictional pressure drop and volumetric flow rates. The average HL contour at the flowline cross-section is expressed in Fig. 11 and it shows improvement after refining the mesh for flow having Re_{so} values of about 450−2750 and Re_{sw} = 6772. In Fig. 11a, Po/w is observed at Re_{so} of 450 with higher water HL than oil in the continuous water phase. SI & MI is noticed in Fig. 11b as Re_{so} increases above 450 showing almost equal HL of oil and water in the continuous oil-water phases. At Re_{so} lower than 2750 in Fig. 11c, Dw/o & o/w flow regime is observed as the HL of water decreases during the transition which indicated that the dispersed water continuous flow moved much faster than the dispersed oil continuous phase. Additional increase in Re_{so} to approximately 2750 results in Dw/o where HL of water further reduces, which demonstrated that the dispersed water droplets moved faster than the continuous oil phase (Fig. 11d). it can be seen that the water droplet concentration increased towards the flowline midpoint where the velocity is highest. Lift forces were responsible for the increased droplet concentration at the midpoint.

Fig. 12a, b, and 12c describe the liquid holdup for horizontal and inclined flowlines, it is observed as the superficial oil velocity increases at constant water velocity during a transition from Po/w to Dw/o, the in-situ water volume fraction decreases. The Po/w is seen to have a higher water fraction than oil in the continuous water phase with an HL ratio between oil and water to be 0.75 in horizontal flow, 0.94 for upward flow, and 0.82 in a downward flow. This is owing to the gravitational forces acting in the upward flow hindering the denser water phase and increasing the heavy phase HL. ST & MI is noticed at higher oil flow rates with both oil and water having continuous phases, where the HL ratio between oil

Table 6
Oil-water flow patterns at different inclinations.

Flowline Inclinations				
-7°	-4°	0°	+4°	+7°
3D Predict	3D Predict	3D Predict	3D Predict	3D Predict
Po/w	Po/w	Po/w	Po/w	Po/w
ST & MI	ST & MI	ST & MI	ST & MI	ST & MI
ST & MI	ST & MI	Dw/o & o/w	ST & MI	ST & MI
ST & MI	ST & MI	Dw/o & o/w	Dw/o & o/w	Dw/o & o/w
Dw/o & o/w	Dw/o & o/w	Dw/o & o/w	Dw/o & o/w	Dw/o & o/w

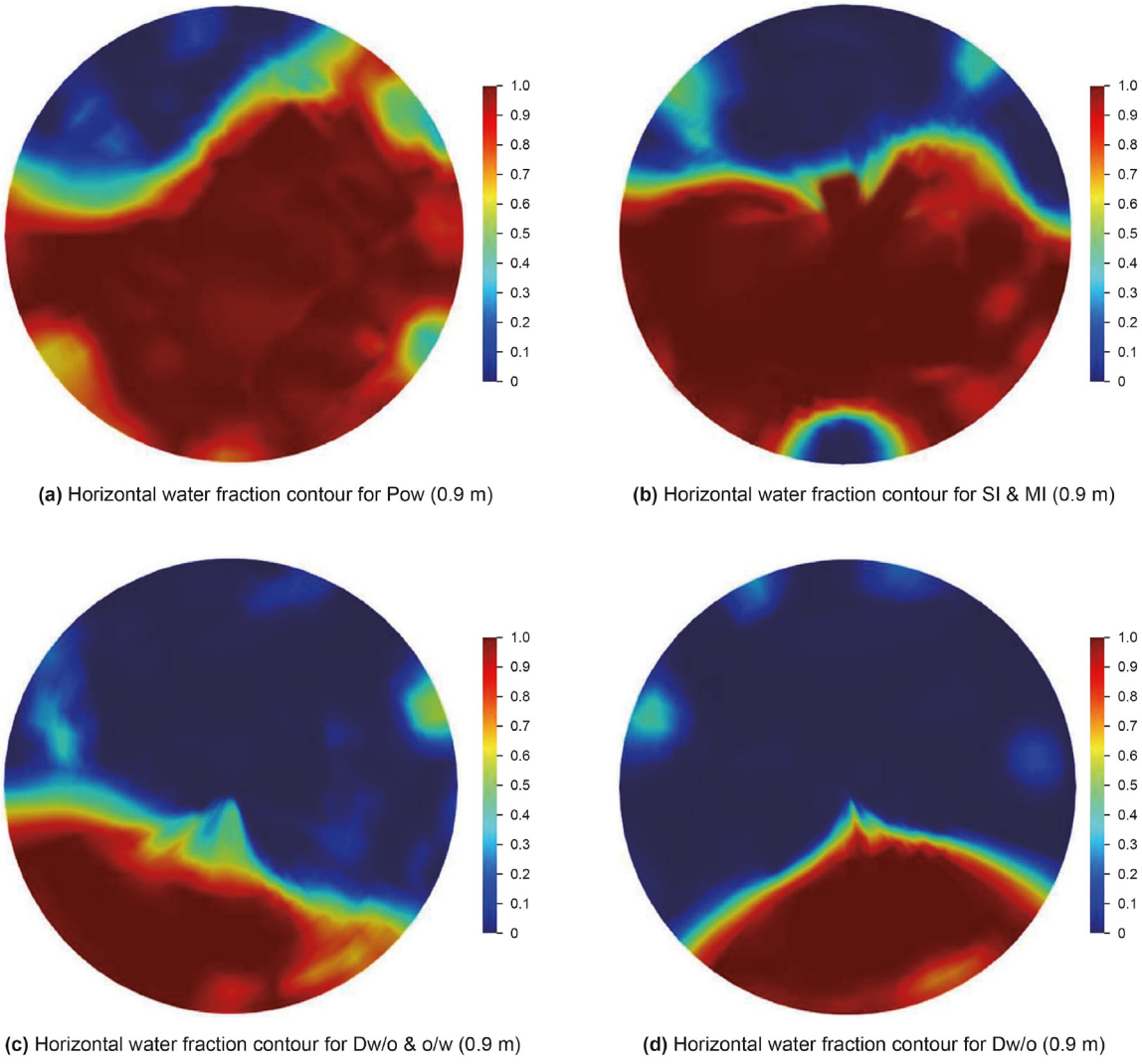

(a) Horizontal water fraction contour for Pow (0.9 m)

(b) Horizontal water fraction contour for SI & MI (0.9 m)

(c) Horizontal water fraction contour for Dw/o & o/w (0.9 m)

(d) Horizontal water fraction contour for Dw/o (0.9 m)

Fig. 11. The liquid fraction variation contour at flowline cross-section maintained at $Re_{sw} = 6772$ for different Re_{so}.

and water is 0.67 in horizontal flow, 0.73 for upward flow, and 0.62 in a downward flow. For high flow rates of dispersed oil flow, where Dw/o & o/w flow is observed to occur. HL ratio between oil and water continuous phases is 0.42 in horizontal flow, 0.51 for upward flow, and 0.45 in a downward flow. Further increase in the dispersed continuous oil flow phase leads to Dw/o being observed. Dw/o has an HL ratio between oil and water of 0.35 in horizontal flow, 0.46 for upward flow, and 0.38 in a downward flow.

Finally, in upward flow, the denser phase decelerates due to gravity forces which increases the heavy phase holdup. Conversely, the velocity of the denser phase in the downward flow increases resulting in a decreased holdup.

4.2.2. Pressure along flowline length

The value of the pressure gradient along the flowline length was investigated at different Re_{so} values (450–2750) while maintaining $Re_{sw} = 6772$ as shown in Fig. 13. It is observed in horizontal flow that the frictional pressure gradient increases in the transition from Po/w to Dw/o flow due to increased turbulence forces (Fig. 13a). Based on Po/w, when the inlet oil flow rate increases, the oil-water flow pattern transition to ST & MI. The pressure variation rose as the water continuous phase in Po/w was replaced with an oil-water

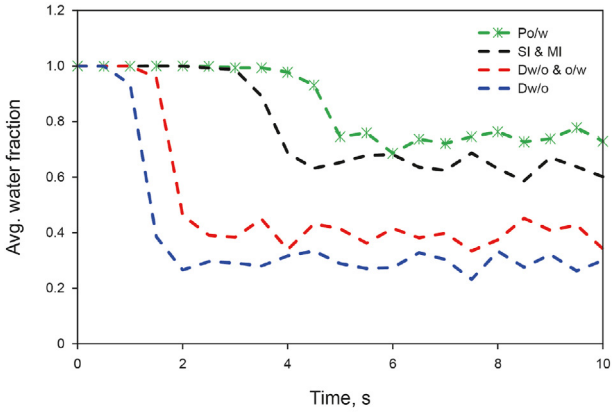

(a) Liquid fraction at a horizontal length of 0.9 m

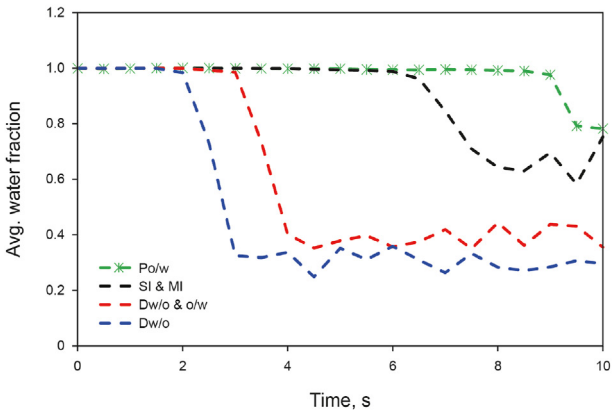

(b) Liquid fraction at the upward inclined length of 0.9 m

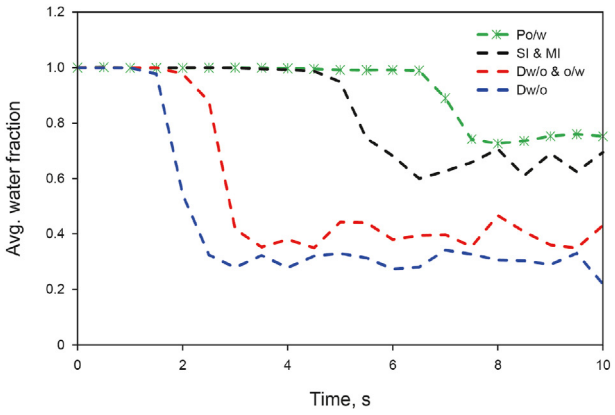

(c) Liquid fraction at the downward inclined length of 0.9 m

Fig. 12. Time step liquid distribution at flowline cross-section for Re_{sw} = 6772 and different values of Re_{so}.

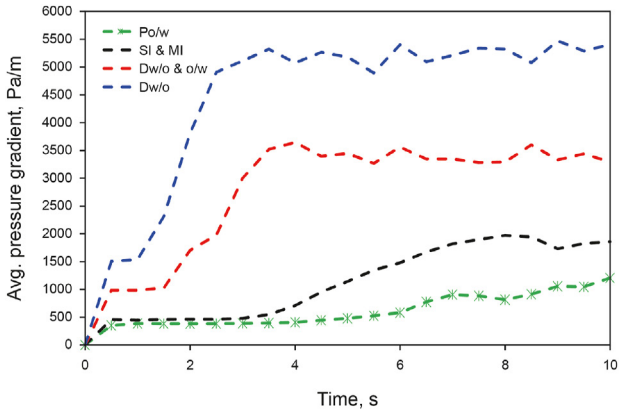

(a) Pressure gradient at the horizontal length of 1.8 m

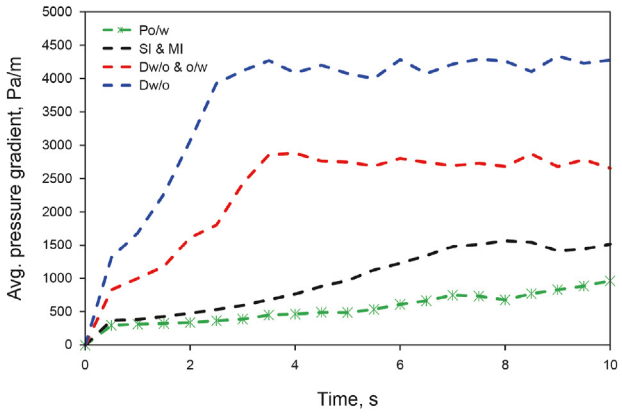

(b) Pressure gradient at an upward inclined length of 1.8 m

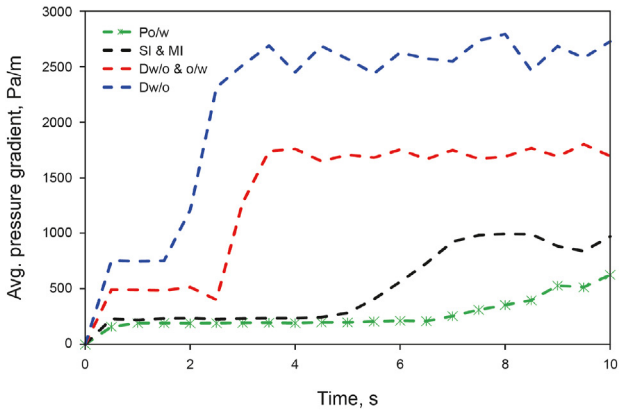

(c) Pressure gradient at a downward inclined length of 1.8 m

Fig. 13. Time series pressure gradient along flowline at different Re_{so} values and Re_{sw} = 6772.

continuous phase, which increases the wall friction and frictional pressure drop. Increasing the oil flow rates, the oil-water flow changes to Dw/o & o/w flow regime, and the pressure variation increases because of the high inlet velocity and the amount of continuous oil-water phases in the flowline. Based upon Dw/o & o/w, a further increase in the inlet oil flow rates, the oil-water flow changes to Dw/o. The pressure gradient further increases as the continuous oi-water phases are substituted with an oil continuous phase, which increases the frictional pressure drop. However, due to the influence of the hilly-terrain flowline as seen in this study in Fig. 13b and c. The frictional pressure gradients at the different flow transitions from Po/w to Dw/o are in general noticed to be lower than horizontal flow. This was ascribed to a higher in-situ water fraction or holdup in the upward and reduced holdup in the downward flows. In essence, confirms the investigations that flow pattern has a big impact on the measured pressure gradient (Trallero, 1995).

In summary, the frictional pressure drop in production flowlines has a huge impact on the operational cost and design. It restricts the maximum flow and hence a critical parameter, during production

optimization and cost evaluation.

4.2.3. Velocity distribution

Fig. 14 shows the midpoint velocity contour of the oil-water phase in a fully developed two-phase flow for different Re_{so} values while Re_{sw} is maintained at 6772. It is observed that a pronounced velocity distribution effect is noticed in the water phase than in the oil phase. The velocity contour of the water phase is higher at the interface and near the flowline wall, this implies that the velocity gradient of the water phase is higher than the oil phase. It is also discovered that the oil-water two-phase velocity decelerates while approaching either the oil-water interface or due to impeding effects of fluid viscosity. The average velocities distribution of Po/w is 0.30 m/s in Fig. 14a, 0.33 m/s for SI & MI (Fig. 14b), 0.57m/s for Dw/o & o/w (Fig. 14c), and 0.75 m/s for Dw/o in Fig. 14d.

4.3. Effect of flowline inclinations on thermal behavior

4.3.1. Temperature variations

The temperature distribution at the midpoint of the flowline cross-section for different inclinations is shown in Fig. 15. As can be seen in the temperature contour, the temperature of both oil and water phases increases because of the higher surrounding temperature through the constant wall heat flux and the convective heat transfer effects. Therefore, as the superficial oil velocity increases at constant water velocity during the transition from Po/w to Dw/o in horizontal flow, the temperature of oil and water keeps increasing from the flowline wall to the fluid interface, and the temperature gradient in the radial direction of the water phase is smaller than that of the oil phase gradient (Fig. 16a). This is because oil has a lower specific heat transfer heat capacity (c_p) than water and the phenomenon entails heat is transferred from the wall to the oil interface faster.

Fig. 16b and c describe the temperature variation along the upward and downward flowline cross-section. The temperature variation is observed to be higher than that of horizontal flow. This was attributed to a higher liquid holdup by gravitational forces in the upward flow and a reduced liquid holdup in the downward flow. From the temperature distribution at the vertical midpoint of the flowline cross-section in Fig. 17, it is obtained that the maximum temperature at the flowline cross-section occurs at the flowline wall and the minimum temperature at the oil-water interface.

4.3.2. HTC

4.3.2.1. HTC Vs. Re_{so}. The numerical HTC results at different Re_{so}

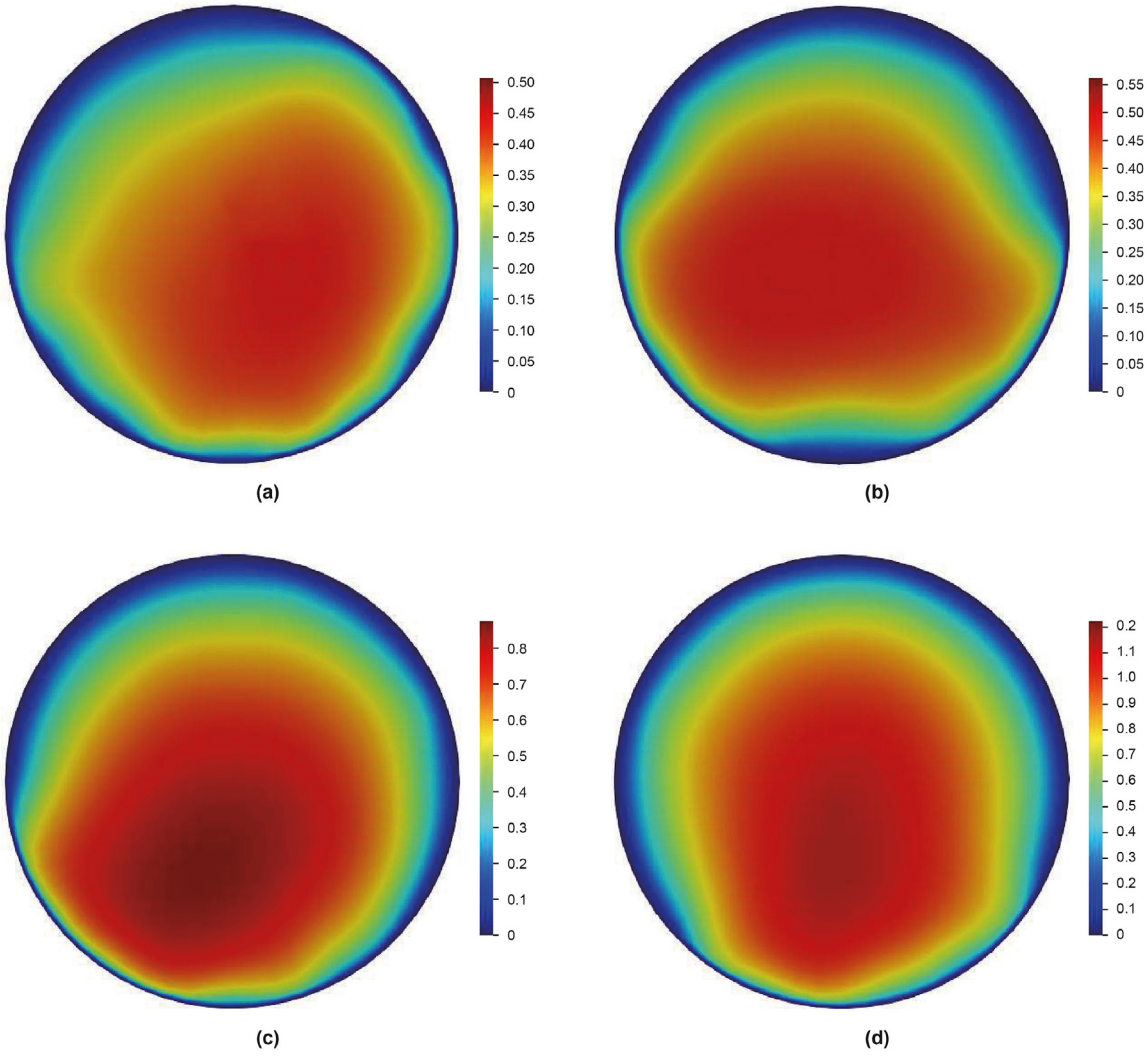

Fig. 14. The midpoint velocity distribution at $Re_{sw} = 6772$ and different Re_{so} for (**a**) Po/w (**b**) SI & MI, and (**c**) Dw/o & o/w (**d**) Dw/o.

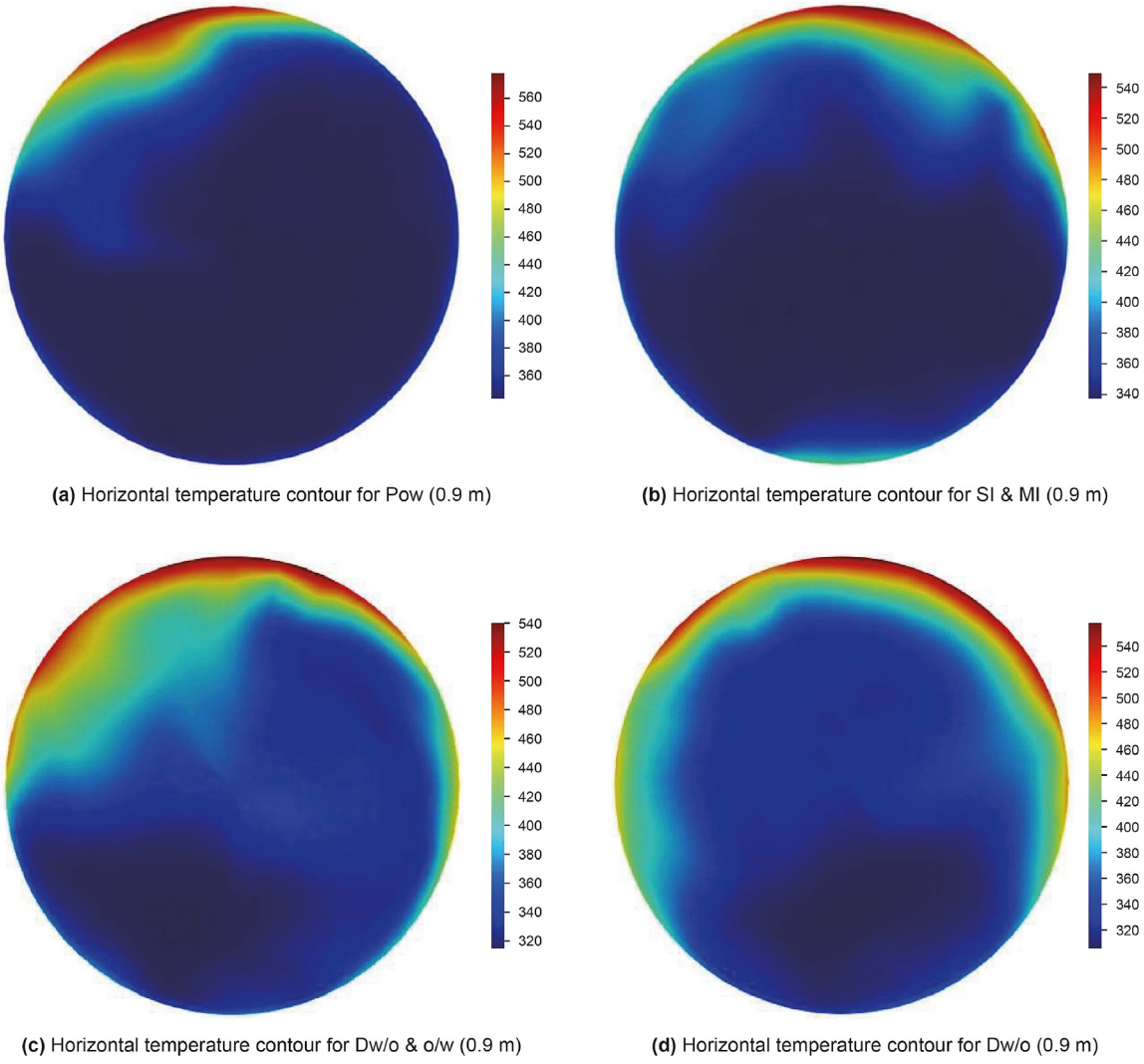

(a) Horizontal temperature contour for Pow (0.9 m)

(b) Horizontal temperature contour for SI & MI (0.9 m)

(c) Horizontal temperature contour for Dw/o & o/w (0.9 m)

(d) Horizontal temperature contour for Dw/o (0.9 m)

Fig. 15. The temperature variation at the flowline cross-section maintained at $Re_{sw} = 6772$ for different Re_{so}.

(about 450−2750), flow patterns, flowline inclinations (-7°, -4°, 0°, +4°, +7°), and Re_{sw} of 6772 are shown in Fig. 18. In downward flows, the flow pattern transition from Po/w to ST & MI regime causes a decrease in HTC values. Further increase in the oil flow rates coupled with gravity forces working in the reverse direction to the upward inclined flow enhances the interfacial mixing of the oil-water flow, resulting in increased overall HTC from ST & MI to Dw/o & o/w. Changing flowline inclination from horizontal to downward flow increases the HTC during flow pattern transition. However, the HTC for horizontal flow is higher than the downward flow at Re_{so} values of about 1200−1800. This difference is traceable to Dw/o & o/w flow pattern observed in horizontal flow and ST & MI for the downward flow at this Re_{so} range. HTC is higher at this range for horizontal flow due to higher turbulence forces in Dw/o & o/w than in ST & MI flow pattern.

4.3.2.2. Average HTC vs. flowline inclination. The comparison of the increase in average HTC between four flow patterns for different flowline inclinations is expressed in Fig. 19. The results were obtained by averaging the HTC values for each flow pattern. From the figure of all four flow patterns, the HTC is noticed to increase with changing flowline inclination angle from 0 to -7° and 0° to +7°. The increase in HTC is more for downward than upward flows due to the gravitational forces. In addition, the increase in HTC for Dw/o & o/w is higher than that for the other flow patterns.

Finally, the proposed numerical model was able to compute the HTC results for two-phase oil-water flows and it is a function of the flow pattern.

5. Conclusions

A quasi-transient state 3D non-isothermal two-phase oil-water flow model is established to explore the complex mechanisms of flow behavior and heat transfer in different flowline inclinations. LRN k-ε is utilized to simulate the turbulence viscosity based on the solution of the momentum conservation and energy conservation equations. The computed results were validated with experimental data in the literature with a relative error of within 3%, which demonstrates the high accuracy of the model. Afterward, a study of non-isothermal oil-water simulations at different flow patterns and flowline inclinations is carried out. Sensitivity analyses were initially conducted using the factorial design method on the model to determine the most relevant parameters of the hydrodynamic and thermal behaviors. The flow patterns, HTC along the flowline at different flow rates, Newtonian behavior, and flowline orientations are predicted. Detailed flow information like liquid holdup,

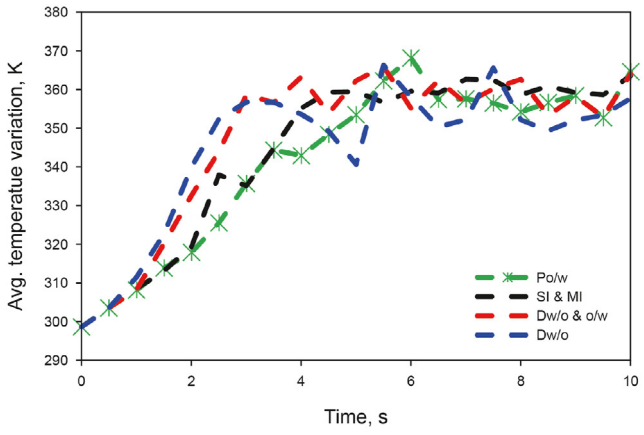

(a) Temperature variation at the horizontal length of 0.9 m

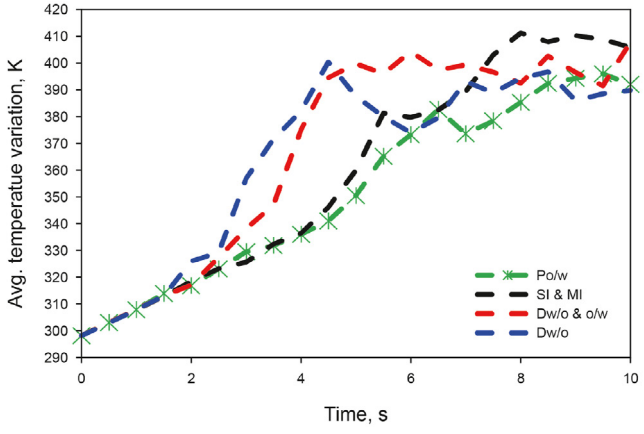

(b) Temperature variation at an upward inclined length of 0.9 m

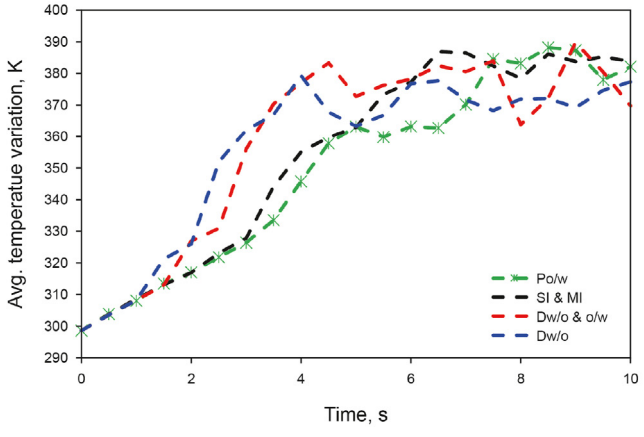

(c) Temperature variation at the downward inclined length of 0.9 m

Fig. 16. Time-series temperature variation at flowline cross-section for Re_{sw} = 6772 and different values of Re_{so}.

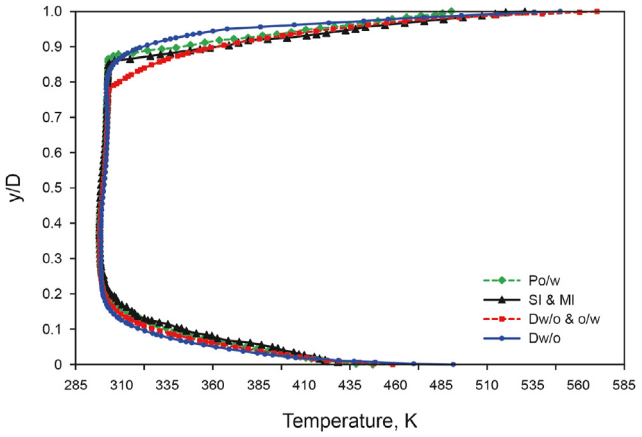

Fig. 17. Temperature distribution at midpoint flowline cross-section (Re_{sw} = 6772 and different Re_{so}).

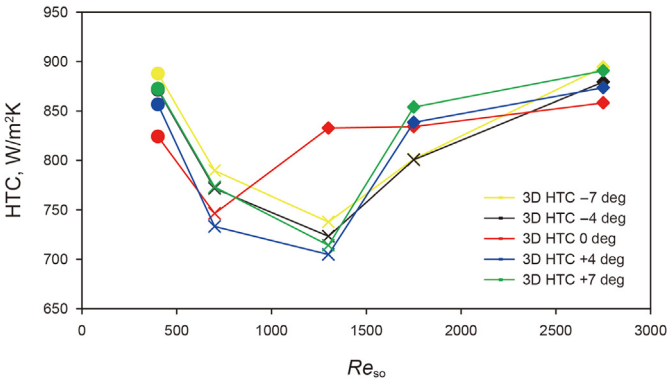

Fig. 18. The HTC variation at different flowline inclinations as a function of Re_{so}.

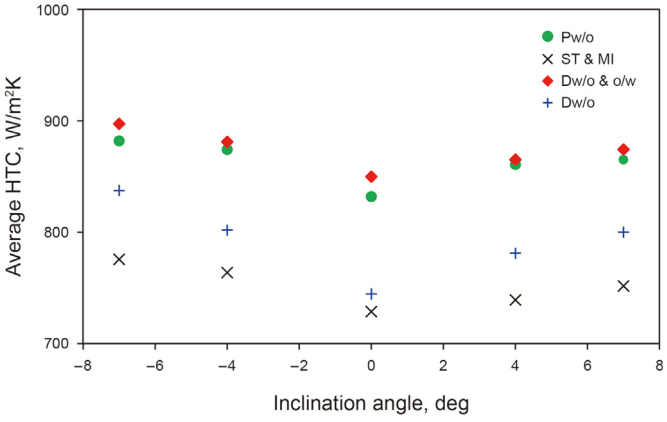

Fig. 19. Effect of average HTC for different flow patterns on the flowline inclination angles.

pressure gradient, velocity distribution, and temperature on flowline cross-sections at different flowline inclinations and flow patterns are investigated. Based on the data considered in this work, the conclusions obtained are:

- The sensitivity analyses of ST and Dw/o flow respectively describing the minimum and maximum flow boundary in the flow pattern map show that flowline inclination, fluid velocity, the thermal conductivity of oil, and wall heat flux are the most relevant parameters affecting the fluid temperature.
- In the horizontal flowline, the in-situ water volume fraction decreases as the oil superficial velocity increases at constant water superficial velocity during a transition from Po/w to Dw/o. For upward flow, the in-situ water volume fraction increases because the denser phase decelerates due to gravity forces.

Conversely, a decreased holdup in the downward flow results from a velocity increase of the denser phase.

- The frictional pressure gradient in the horizontal flowline increases through the transition from Po/w to Dw/o flow. The pressure drops rose as the water continuous phase was replaced with an oil continuous phase, which increases the wall friction. The frictional pressure gradients in upward and downward flows decrease due to a higher in-situ water fraction or holdup.
- A pronounced velocity distribution effect is noticed in the water phase than in the oil phase. The velocity contour of the water phase is higher at the interface and near the flowline wall which suggests that the velocity gradient of the water phase is higher than the oil phase. Also, oil-water two-phase velocity slows down while approaching either the oil-water interface or by the hindering effects of fluid viscosity.
- The average temperature of the two-phase oil-water horizontal flowline increases from the wall to the fluid interface, and the temperature gradient in the radial direction of the water phase is smaller than that of the oil phase gradient. In upward flow, the temperature is higher than that of horizontal flow due to a higher liquid holdup by gravitational forces in the upward flow.
- Changing flowline inclination from horizontal to downward and upward flows increases the HTC during flow pattern transition. Nevertheless, the HTC for horizontal flow is higher than the downward and upward flows at Re_{so} values of about 1200–1800. This is owing to higher turbulence forces in Dw/o & o/w than in ST & MI flow patterns in upward and downward flows.

Consequently, the numerical model we proposed could be generally applied to compute the global fluid properties and other operating variables in the two-phase oil-water flowlines transportation system.

Acknowledgments

The authors express heartfelt appreciation to the Petroleum Technology Development Fund (PTDF) of Nigeria for funding the Ph.D. thesis at PRISME Laboratory INSA Centre Val de Loire, Bourges- France.

References

Abduvayt, P., Manabe, R., Watanabe, T., Arihara, N., 2004. Analisis of oil-water flow tests in horizontal, hilly-terrain, and vertical pipes. In: SPE Annual Technical Conference and Exhibition. OnePetro.

Abubakar, A., Al-Hashmi, A.R., Al-Wahaibi, T., Al-Wahaibi, Y., Al-Ajmi, A., Eshrati, M., 2015. Performance of a drag-reducing polymer in horizontal and downward-inclined oil-water flow. Chem. Eng. Res. Des. 104, 237–246.

Adesina, F.A., Churchill, A., Olugbenga, F., 2011. Modeling productivity index for long horizontal well. J. Energy Resour. Technol. 133.

Akridiss Abed, S., Settar, A., Chetehouna, K., Kadiri, M.S., El Tabach, E., Gascoin, N., 2020. Numerical study on a porous material subject to SiC particles deposition, using OpenFOAM and sensitivity analysis technique: effect of clogging evolution on the thermal performances. Chem. Eng. Sci. 212, 115321. https://doi.org/10.1016/j.ces.2019.115321.

Amundsen, L., 2011. An Experimental Study of Oil-Water Flow in Horizontal and Inclined Pipes (Ph.D. Thesis). Norwegian University of Science and Technology.

Bell, E., Lu, Y., Daraboina, N., Sarica, C., 2021. Thermal methods in flow assurance: a review. J. Nat. Gas Sci. Eng. 88, 103798. https://doi.org/10.1016/j.jngse.2021.103798.

Boostani, M., Karimi, H., Azizi, S., 2017. Heat transfer to oil-water flow in horizontal and inclined pipes: experimental investigation and ANN modeling. Int. J. Therm. Sci. 111, 340–350. https://doi.org/10.1016/j.ijthermalsci.2016.09.005.

Charles, Y.O., Igbokoyi, A.O., 2012. Temperature prediction model for flowing distribution in wellbores and pipelines. In: All Days. Presented at the Nigeria Annual International Conference and Exhibition, SPE, Lagos, Nigeria. https://doi.org/10.2118/163038-MS. SPE-163038-MS.

Choi, J., Pereyra, E., Sarica, C., Lee, H., Jang, I.S., Kang, J., 2013. Development of a fast transient simulator for gas-liquid two-phase flow in pipes. J. Petrol. Sci. Eng. 102, 27–35. https://doi.org/10.1016/j.petrol.2013.01.006.

Duan, J., Gong, J., Yao, H., Deng, T., Zhou, J., 2014. Numerical modeling for stratified gas-liquid flow and heat transfer in pipeline. Appl. Energy 115, 83–94. https://doi.org/10.1016/j.apenergy.2013.10.050.

Duan, J., Liu, H., Gong, J., Jiao, G., 2015. Heat transfer for fully developed stratified wavy gas-liquid two-phase flow in a circular cross-section receiver. Sol. Energy 118, 338–349. https://doi.org/10.1016/j.solener.2015.05.023.

Duan, J., Wang, W., Deng, D., Zhang, Y., Liu, H., Gong, J., 2013. Predicting temperature distribution in the waxy oil-gas pipe flow. J. Petrol. Sci. Eng. 101, 28–34. https://doi.org/10.1016/j.petrol.2012.10.003.

Ekweribe, C., Civan, F., 2011. Transient wax gel formation model for shut-in subsea pipelines. J. Energy Resour. Technol. 133.

Farshad, F.F., Garber, J.D., Lorde, J.N., 2000. Predicting temperature profiles in producing oil wells using artificial neural networks. Eng. Comput. 17 (6), 735–754. https://doi.org/10.1108/02644400010340651.

Ghajar, A.J., Tang, C.C., 2010. Importance of non-boiling two-phase flow heat transfer in pipes for industrial applications. Heat Tran. Eng. 31, 711–732. https://doi.org/10.1080/01457630903500833.

Ghajar, A.J., Tang, C.C., 2007. Heat transfer measurements, flow pattern maps, and flow visualization for non-boiling two-phase flow in horizontal and slightly inclined pipe. Heat Tran. Eng. 28, 525–540. https://doi.org/10.1080/01457630701193906.

Guo, B., Duan, S., Ghalambor, A., 2006. A simple model for predicting heat loss and temperature profiles in insulated pipelines. SPE Prod. Oper. 21, 107–113.

Hall, J.W., Boyce, S.A., Wang, Y., Dawson, R.J., Tarantola, S., Saltelli, A., 2009. Sensitivity analysis for hydraulic models. J. Hydraul. Eng. 135, 959–969. https://doi.org/10.1061/(ASCE)HY.1943-7900.0000098.

Hamad, F.A., Albarzenji, D., Ganesan, P.B., 2014. Study of kerosene-water two-phase flow characteristics in vertical and inclined pipes. Can. J. Chem. Eng. 92, 905–917.

Hetsroni, G., Mewes, D., Enke, C., Gurevich, M., Mosyak, A., Rozenblit, R., 2003. Heat transfer to two-phase flow in inclined tubes. Int. J. Multiphas. Flow 29, 173–194. https://doi.org/10.1016/S0301-9322(02)00132-5.

Hetsroni, G., Yi, J.H., Hu, B.G., Mosyak, A., Yarin, L.P., Ziskind, G., 1998. Heat transfer in intermittent air-water flows-Part II: upward inclined tube. Int. J. Multiphas. Flow 24, 189–212.

Hirt, C.W., Nichols, B.D., 1981. Volume of fluid (VOF) method for the dynamics of free boundaries. J. Comput. Phys. 39, 201–225. https://doi.org/10.1016/0021-9991(81)90145-5.

Ji, Y., Homan, K.O., 2007. On Simplified Models for the Rate-And Time-dependent Performance of Stratified Thermal Storage.

Jia, W., Yang, F., Mu, J., Cheng, T., Li, C., Zhang, Q., 2019. A multiphase choke temperature model for high-pressure gas/water/glycol mixtures. In: International Petroleum Technology Conference. OnePetro.

Kim, J., Ghajar, A.J., 2006. A general heat transfer correlation for non-boiling gas-liquid flow with different flow patterns in horizontal pipes. Int. J. Multiphas. Flow 32, 447–465. https://doi.org/10.1016/j.ijmultiphaseflow.2006.01.002.

Kumara, W.A.S., Halvorsen, B.M., Melaaen, M.C., 2010. Single-beam gamma densitometry measurements of oil-water flow in horizontal and slightly inclined pipes. Int. J. Multiphas. Flow 36, 467–480.

Launder, B.E., Sharma, B.I., 1974. Application of the energy-dissipation model of turbulence to the calculation of flow near a spinning disc. Lett. Heat Mass Tran. 1, 131–137.

Launder, B.E., Spalding, D.B., 1972. Lectures in Mathematical Models of Turbulence.

Legan, R.W., Knudsen, J.G., 1966. Momentum and heat transfer characteristics of liquid-liquid dispersions in turbulent flow. Can. J. Chem. Eng. 44, 270–275.

Leib, T.M., Fink, M., Hasson, D., 1977. Heat transfer in vertical annular laminar flow of two immiscible liquids. Int. J. Multiphas. Flow 3, 533–549.

Li, Y., He, G., Sun, L., Ding, D., Liang, Y., 2018. Numerical simulation of oil-water non-Newtonian two-phase stratified wavy pipe flow coupled with heat transfer. Appl. Therm. Eng. 140, 266–286. https://doi.org/10.1016/j.applthermaleng.2018.05.048.

Lum, J.-L., Al-Wahaibi, T., Angeli, P., 2006. Upward and downward inclination oil-water flows. Int. J. Multiphas. Flow 32, 413–435.

Mehrotra, A.K., Ehsani, S., Haj-Shafiei, S., Kasumu, A.S., 2020. A review of heat-transfer mechanism for solid deposition from “waxy” or paraffinic mixtures. Can J. Chem. Eng. CJCE 23829. https://doi.org/10.1002/cjce.23829.

Moran, H.R., Zogg, D., Voulgaropoulos, V., Van den Bergh, W.J., Dirker, J., Meyer, J.P., Matar, O.K., Markides, C.N., 2021. An experimental study of the thermohydraulic characteristics of flow boiling in horizontal pipes: linking spatiotemporally resolved and integral measurements. Appl. Therm. Eng. 194, 117085. https://doi.org/10.1016/j.applthermaleng.2021.117085.

Mukherjee, H., Brill, J.P., Beggs, H.D., 1981. Experimental Study of Oil-Water Flow in Inclined Pipes.

Oddie, G., Shi, H., Durlofsky, L.J., Aziz, K., Pfeffer, B., Holmes, J.A., 2003. Experimental study of two and three phase flows in large diameter inclined pipes. Int. J. Multiphas. Flow 29, 527–558. https://doi.org/10.1016/S0301-9322(03)00015-6.

Rodriguez, O.M.H., Baldani, L.S., 2012. Prediction of pressure gradient and holdup in wavy stratified liquid-liquid inclined pipe flow. J. Petrol. Sci. Eng. 96, 140–151.

Rodriguez, O.M.H., Oliemans, R.V.A., 2006. Experimental study on oil-water flow in horizontal and slightly inclined pipes. Int. J. Multiphas. Flow 32, 323–343.

Sagar, R., Doty, D.R., Schmidt, Z., 1991. Predicting temperature profiles in a flowing well. SPE Prod. Eng. 6, 441–448. https://doi.org/10.2118/19702-PA.

Saltelli, A., Tarantola, S., Campolongo, F., Ratto, M., 2004. Sensitivity Analysis in Practice: a Guide to Assessing Scientific Models. Chichester, England.

Shahdi, A., Panacharoensawad, E., 2019. SP-Wax: solid-liquid equilibrium

thermodynamic modeling software for paraffinic systems. SoftwareX 9, 145–153. https://doi.org/10.1016/j.softx.2019.01.015.

Shang, W., Sarica, C., 2013. A model for temperature prediction for two-phase oil/water stratified flow. J. Energy Resour. Technol. 135, 032906. https://doi.org/10.1115/1.4023931.

Singh, A., Panacharoensawad, E., Sarica, C., 2017. A mini pilot-scale flow loop experimental study of turbulent flow wax deposition by using a natural gas condensate. Energy Fuel. 31, 2457–2478. https://doi.org/10.1021/acs.energyfuels.6b02125.

Somer, T.G., Bora, M., Kaymakçalan, Ö., Özmen, S., Arikan, Y., 1973. Heat transfer to an immiscible liquid mixture and between liquids in direct contact. Desalination 13, 231–249.

Sözbir, N., 2006. A New Approach to the Simulation of Thermal Systems.

Stockman, G.E., Epstein, N., 2001. Uniform flux heat transfer in concentric laminar flow of two immiscible liquids. Can. J. Chem. Eng. 79, 990–994.

Sunday, N., Settar, A., Chetehouna, K., Gascoin, N., 2021. An overview of flow assurance heat management systems in subsea flowlines. Energies 14, 458. https://doi.org/10.3390/en14020458.

Sunday, N., Settar, A., Chetehouna, K., Gascoin, N., 2022a. Numerical study and sensitivity analysis of two-phase oil-water flow and heat transfer in different flowline orientations using OpenFOAM. Case Stud. Therm. Eng. 40, 102465. https://doi.org/10.1016/j.csite.2022.102465.

Sunday, N., Settar, A., Chetehouna, K., Gascoin, N., 2022b. Numerical heat transfer analysis of two-phase flow in horizontal and inclined flowline using OpenFOAM. In: ICHMT DIGITAL LIBRARY ONLINE. Begel House Inc.

Toma, P., Ivory, J., Korpany, G., derocco, M., Holloway, L., Goss, C., Ibrahim, J., Omar, I., 2006. A Two-Layer Paraffin Deposition Structure Observed and Used to Explain the Removal and Aging of Paraffin Deposits in Wells and Pipelines.

Trallero, J.L., 1995. Oil-water Flow Patterns in Horizontal Pipes (PhD. Thesis). The University of Tulsa, Tulsa, OK.

Trimble, S., Kim, J., Ghajar, A.J., 2002. Experimental heat transfer comparison in air-water slug flow in a slightly upward inclined tube. In: International Heat Transfer Conference Digital Library. Begel House Inc.

Vianna, F.L.V., Orlande, H.R.B., Dulikravich, G.S., 2009a. Prediction of the temperature field in pipelines with Bayesian filters and non-intrusive measurements. In: Proceedings of the 20th International Congress of Mechanical Engineering, Gramado, RS, Brazil. Citeseer.

Vianna, F.L.V., Orlande, H.R.B., Dulikravich, G.S., 2009b. Estimation of the temperature field in pipelines by using the Kalman filter. In: Proceedings of the 2nd International Congress of Serbian Society of Mechanics (IConSSM 2009), Palic (Subotica), Serbia. Citeseer, pp. 1–5.

Wilcox, D.C., 2006. Turbulence Modeling for CFD. DCW Industries. Inc, November, La Canada, CA.